The Role of the Blend Interface Type on Morphology in Cocontinuous Polymer Blends

Jianming Li, Pei Lian Ma, and Basil D. Favis*

Çentre de Recherche Appliquée Sur les Polymères (CRASP), Département de Génie Chimique, École Polytechnique de Montréal, P.O. Box 6079 Station Centre-Ville, Montréal, (QC) Canada H3C 3A7

Received January 22, 2001

ABSTRACT: Three different categories of blend interfaces are examined systematically in order to isolate the role of the interface in the development of cocontinuous morphologies during melt mixing. They are Type I, compatible binary blends based on high-density polyethylene (HDPE)/styrene−ethylene−butylene−styrene (SEBS) and HDPE/styrene−ethylene−butylene (SEB); Type II, an incompatible binary system comprised of HDPE/polystyrene (PS); and Type III, compatible ternary systems comprised of HDPE/PS compatibilized by SEBS in one case and by SEB in another. The Type I and Type III systems represent conventional approaches to preparing blend systems of low interfacial tension. The cocontinuous morphology is analyzed using three techniques: microscopy/image analysis, solvent extraction/gravimetric analysis, and BET characterization of surface area and pore size. A mechanism for the formation of dual-phase continuity based on droplet and fiber lifetimes during melt mixing has been proposed. For the Type I compatible binary systems continuity development and microstructural features are dominated by thread−thread coalescence. In the Type II incompatible HDPE/PS binary system and Type III compatibilized ternary systems, continuity development and microstructural features are controlled by droplet−droplet coalescence and reduced droplet−droplet coalescence, respectively. In the latter case, the generation of fresh interface during droplet deformation results in a system that is only partially emulsified. The relative presence of fibers or droplets during dynamic mixing is analyzed quantitatively using a matrix dissolution/image analysis technique. A thread frequency ratio (TFR) is proposed as a basic general parameter to classify the relative presence of fibers to droplets during mixing and hence the type of continuity development for a given system.

1. Introduction

When melt blending immiscible polymers, two major categories of morphologies are possible: a dispersed phase/matrix or a cocontinuous morphology. At compositions above the percolation threshold, various levels of continuity exist. Cocontinuity is a special case of blend morphology in which each polymer is fully interconnected through a continuous pathway. Recently, much interest has been generated in polymer blends with a cocontinuous morphology[1−15] due to a number of promising applications.[16−18]

One of the challenges in studying cocontinuous systems is the use of appropriate characterization techniques. In the past, a significant amount of work used only microscopy as the principal method of analysis. Over the past 10 years, however, it has become routine to combine microscopy with extraction/gravimetric analysis as a route to quantifying the level of continuity in a given system. This approach is quite rigorous at estimating the level of continuity but does not provide any quantitative information on the scale of the cocontinuous microstructure. Recently, it has been proposed in this laboratory that BET analysis should be included as a necessary third technique toward the quantification of cocontinuous structures.[7] It has been shown that the BET technique can be used to analyze the complex microstructure of cocontinuous HDPE/PS blends following the extraction of the PS phase. Both the surface area and the pore size are estimated. Using this approach, it has been possible to quantify the emulsification efficacy of an added interfacial modifier in the HDPE/PS dual-phase continuous region. An emulsification curve, virtually similar in form to those observed in conventional droplet−matrix blend systems, is obtained.

Most studies on cocontinuity have been carried out on immiscible binary blends with an emphasis on the role of the viscosity ratio in determining the position of phase inversion.[1,2,8−11] Very little work has been directed toward the role of the interface on cocontinuous morphologies. Bourry and Favis[4] have shown that a compatible ternary blend demonstrated an onset of percolation phenomena and continuity development at higher concentrations than the noncompatible binary blend. Willemse et al.[12] and Veenstra et al.[13] have recently shown that the cocontinuous morphology in a low interfacial tension homopolymer/copolymer system demonstrated low percolation thresholds and persisted over a wide composition range. These effects were related to the formation of very stable elongated structures which do not show breakup during processing. Verhoogt et al.[19] also demonstrated that binary blends of low interfacial tension could possess a wide region of dual-phase continuity.

It is well-known that a reduction of interfacial tension leads to the stabilization of capillary instabilities.[5,20−22] It is reasonable therefore that low interfacial tension binary blends should demonstrate more stable elongated structures during melt mixing and hence a wide region of dual-phase continuity. It becomes more difficult, however, in light of the above, to explain why a number of papers[4,23] have indicated that compatibilized ternary blends, of apparently low interfacial tension, demonstrate a narrower region of dual-phase continuity and

* To whom all correspondence should be addressed.

10.1021/ma010104+ CCC: $22.00
Published on Web 02/07/2002

Table 1. Characteristic Properties of the Materials

	polystyrene	polyethylene	SEBS1	SEBS2	SEB1	SEB2
M_w	215000	79000				
M_n	100000	24000	$S = 7500$ EB = 35000	$S = 3000$ EB = 39000	$S = 20000$ EB = 47000	$S = 48620$ EB = 138,380
density (20 °C), g/mL	1.04	0.962	0.910	0.910	0.910	0.910
density (195 °C), g/mL	0.974	0.754	0.820	0.820	0.820	0.850
supplier	Dow	Dow	Shell	Shell	Shell	Shell

delayed percolation phenomena than their high interfacial tension, incompatible binary blend counterparts. These latter systems appear to display anomalous behavior.

There is clearly a need to formulate a general conceptual mechanism of continuity development for the full range of possible polymer blend interfaces. Furthermore, what is the influence of the interface on the scale of the cocontinuous microstructure itself? The objective of this work is to carry out a broad systematic study to contribute toward a general understanding of the role of the interface on continuity development in polymer blends. Both the continuity development and microstructural features are studied in detail for the three main categories of possible blend interfaces: (I) compatible binary blends, (II) incompatible binary blends, and (III) compatible ternary blend systems.

2. Experimental Procedure

2.1. Materials. The high-density polyethylene (HDPE) and polystyrene (PS) used in this study were obtained from Dow Chemical of Canada. The copolymers were obtained from Shell USA. Kraton G1652 is a triblock copolymer of (styrene)−(ethylene−butylene)−(styrene) designated in this work as SEBS1, with a molecular weight of 35 000 for the center block and 7500 for the PS blocks. Its composition is 30% PS. Cap 2825 is another triblock copolymer of (styrene)−(ethylene−butylene)−(styrene) (SEBS2), with a molecular weight of 39 000 for the center block and 3000 for the PS blocks. Its composition is 13% PS. Two diblock copolymers were used in the study. One is Cap 4741, a diblock copolymer of (styrene)−(ethylene−butylene) (SEB1), with a molecular weight of 47 000 for the (ethylene−butylene block) and 20 000 for the styrene block. Its composition is 30% PS. Another diblock copolymer is a Cap 4745 (SEB2) containing 26% PS, with a molecular weight of 138 380 for the EB block and 48 620 for the PS block. The properties of the materials are listed in Table 1.

2.2. Breaking Thread Method. The measurement of the interfacial tension was carried out using the breaking thread method. It is based on theories developed first by Lord Rayleigh [24] and later by Tomotika.[25] This method consists of sandwiching a thin filament between two films of the matrix, taking it up to temperature and examining the development of capillary instabilities. In the molten state, the distortions generated in the thread start to grow at the interface. The expression of interfacial tension is given by

$$\sigma = \frac{q\eta_m D_0}{\Omega_m} \tag{1}$$

where q is the growth rate of the distortion, η_m is the viscosity of matrix, D_0 is the initial thread diameter, and Ω_m is a tabulated function, which is related to both viscosity ratio and the wavelength of the distortion, and can be calculated from Tomotika's original equations. This method has been reported in more detail in a number of previous papers.[5,20−22]

2.3. Rheology. The polymers were pressed at 195 °C in order to obtain the disks used for the rheological measurement. Rheological characterization of the specimens was carried out using a Bohlin constant stress rheometer (CSM) in the dynamic mode at 195 °C under a nitrogen atmosphere and in the range of 0.01−30 Hz frequency with a strain of 5%. A parallel-plate configuration was used with a gap about 1.4 mm. The Cox−Merz rule is applicable to the materials measured.[13,26]

2.4. Blend Preparation. Binary blends and compatibilized ternary blends were prepared by melt mixing the polymers in a Brabender mixer, which is predominantly a shear mixing device. Compatible and noncompatible blends were prepared over the total composition range with steps of 10 vol %. For the compatible ternary blend system the melt blending was carried out in two steps. In the first step the copolymer was melt blended with the minor component. The second step consisted of melt blending the minor component (containing copolymer) with the matrix. A typical blending experiment consists of the following steps. With the temperature of the mixing chamber initially set at 195 °C and blades turning at 50 rpm, the resin mixture was fed into the chamber. Once all of the resin was added, the blend was allowed to mix for 5 min under a constant flow of dry nitrogen. Next, the melt was rapidly dropped into a bath of liquid nitrogen for 3 min to freeze in the morphology.

In all the compatible ternary blend systems the volume percent of copolymer compatibilizer used is 20% based on the minor phase.

2.5. Microscopy and Image Analysis. Prior to microscopic observation, the samples were microtomed under liquid nitrogen to create a plane face using a Reichert Jung Supercut 2050 equipped with a glass knife. While cutting, the surface of the sample was held at approximately −150 °C to reduce the degree of surface deformation. The microtomed samples were then treated with THF in a Soxhlet extractor to dissolve one of the phases to obtain better contrast. Finally, the samples were coated with gold and palladium and observed under a JEOL JSM 840 scanning electron microscope operated at a working voltage of 10 or 15 kV.

For the dispersed phase in the composition of 30% and below, a semiautomatic method of image analysis consisting of a digitizing table and an in-house software was used to quantify the dispersed phase morphology. The number-average, d_n, and volume-average diameters, d_v, were obtained from the measurement of at least 200 diameters. Since the microtome does not necessarily cut the dispersed phase at the equator and since it is necessary to correct for polydispersity, a correction was applied in order to obtain the true diameter.[27] The maximum error for the measurement of d_n and d_v is about ±10%. In the case of compatibilized or low interfacial tension systems this error reduces to about ±5%.

2.6. Solvent Extraction. Extraction of the dispersed phase was performed in a Soxhlet extraction apparatus

$$\%\ \text{continuity} = \frac{(\text{wt of copolymer or PS})_{\text{initial}} - (\text{wt of copolymer or PS})_{\text{final}}}{(\text{wt of copolymer or PS})_{\text{initial}}} \times 100 \tag{2}$$

with tetrahydrofuran (THF) for 36 h. A gravimetric method was used to calculate the extent of continuity of the removed phase (PS or copolymers) based on eq 2. In the compatibilized ternary blend all the copolymer is considered to be extracted with the PS. This is clearly the case since the THF is very effective at dissolving out all the copolymer in the binary compatible blend systems. In this paper cocontinuity in an A/B blend system can be defined as the concentration range where both A and B phases are 100% continuous. The maximum error for the continuity measurement is ±5%. Further details are given in previous work.[7]

2.7. BET Measurement. On removing one of the phases by solvent extraction, the sample becomes a porous material. A flowsorb BET (Brunauer, Emmett, and Teller) instrument was used to measure the surface area and pore size of the extracted samples. Prior to testing, a given amount of nitrogen gas was introduced to the instrument through a septum to calibrate the system. Sample testing was conducted at liquid nitrogen temperature. The nitrogen gas continuously passes through the sample cell. When the sample cell is immersed into and removed from the liquid nitrogen bath, adsorption and desorption of nitrogen gas occur on the sample surface. Room temperature water was used to warm the sample tube to accelerate the desorption process. Adsorption and desorption data were recorded during the test. The BET technique measures the total volume of nitrogen gas adsorbed on the surface, v, which can be converted to the volume of nitrogen gas required to form an adsorbed monomolecular layer, v_m.[7] The surface area of the sample, S, is then calculated from

$$S = v_m N a / V_M \quad (3)$$

where N is Avogadro's number, a is the area of one adsorbed nitrogen molecule (16.2×10^{-20} m^2), and V_M is the molar volume of the gas. Two assumptions were made for the estimation of the pore diameter: (1) the pores in the sample can be taken as an interconnected cylinder, and (2) only the surface of the pore wall is considered. With the above assumptions the pore diameter, d, may be estimated by

$$d = 4V/S \quad (4)$$

where V is the total volume of the pore in the sample. The total time for the test is about 30 min. The maximum error for the surface area measurement is about ±5%. Further details of this technique are given in previous work.[7]

Bulk polyethylene samples were tested in order to correct for the case of nitrogen absorption by HDPE. However, no absorption was registered by the apparatus under the same testing conditions as above.

2.8. Matrix Dissolution Technique. To determine the shape (fiber or droplet) of the dispersed phase during mixing, the extraction of the matrix (PS or copolymer) in the mixed blend was performed followed by centrifugation and in some cases filtration. Initially, the blend sample (about 1 g) was placed into a centrifuge tube filled with 50 mL of THF. The tube containing the sample was then placed on a shaker for 48 h. It was then centrifuged for 1 h. The solution was poured away, fresh solvent was added to wash the precipitated HDPE, and the sample was shaken again. This process was repeated three times which was sufficient to separate the HDPE dispersed phase from PS for the HDPE/PS and HDPE/PS/SEBS1 blends. The solution of the latter was slightly translucent in color. It was difficult to remove all the copolymer matrix from the 5HDPE/95SEBS blend. In this case the sample solution was diluted to 1/10 of its original concentration and was then subjected to a filtration process. Finally, all the dispersed phase samples were carefully collected and dried in a vacuum oven for 72 h at 40 °C.

After the matrix dissolution technique described above, a TFR measurement based on eq 7 was undertaken for the dispersed phase obtained after matrix extraction. Five fields of view taken using the SEM and approximately 500 particles and threads were considered for a given sample. The tf (thread frequency) and the df (droplet frequency) were obtained by counting the number of each respective species. A droplet was considered to be a thread once it exceeded an aspect ratio of 3.

3. Results and Discussion

3.1. Rheology. Figure 1 shows the complex viscosity as a function of frequency for the raw materials used. These materials follow the Cox−Merz rule so that the shear rate dependence of the steady state viscosity is equal to the frequency dependence of the linear viscoelastic viscosity. The HDPE and PS show shear thinning behavior over almost the complete range of measured frequencies, and Newtonian flow behavior is only observed at the lowest frequencies. The viscosities of triblock copolymer SEBS1 (containing 30% styrene) and diblock copolymer SEB1 (containing 30% styrene) are higher than those of polyethylene and polystyrene for the whole range of frequencies. SEBS1 displays the highest complex viscosity. There was no Newtonian behavior observed in the whole experimental frequency range for SEBS1 and SEB1. However, the SEBS2 displayed a Newtonian plateau at low frequencies and shear thinning behavior at higher frequencies. The complex viscosity of SEBS2 is lower than those of HDPE and PS. Figure 2 illustrates the storage moduli of HDPE, PS, SEBS1, SEBS2, and SEB1. The storage moduli of SEBS1 and SEB1 is higher than those of HDPE and PS, while the storage modulus of SEBS2 is lower than those of HDPE and PS. The viscosity and elasticity ratios of all the blends studied are given in Table 2. It will be demonstrated below that 50 rpm in the internal mixer corresponds to an average shear rate of 50 s^{-1}.

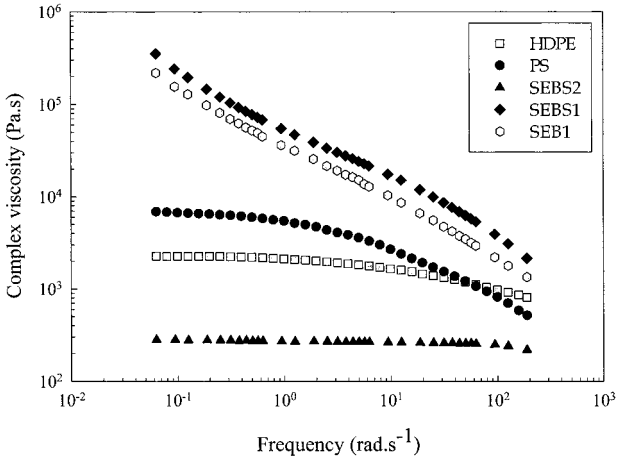

Figure 1. Complex viscosity−frequency relationship for SEB1, SEBS1, SEBS2, HDPE, and PS at 195 °C.

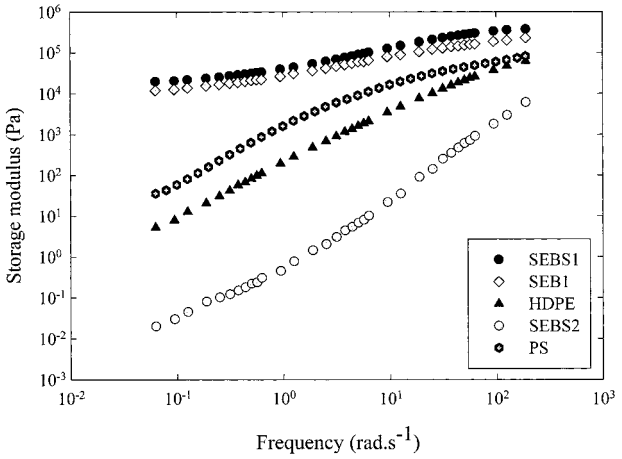

Figure 2. Storage modulus−frequency relationship for SEB1, SEBS1, SEBS2, HDPE, and PS at 195 °C.

To estimate the appropriate viscosity and elasticity ratios for the HDPE and PS in the mixing chamber, a torque study of the pure components was carried out in the Brabender mixer. Previous studies from this laboratory[28] have clearly shown that the torque ratio (torque of PS/torque of HDPE) from the Brabender mixer can

Table 2. Viscosity and Elasticity Ratios for All Blends Studied (T = 195 °C)[a]

	η^* (Pa·s)	η^*_d/η^*_{HDPE}	G' (Pa)	G'_d/G'_{HDPE}	torque (N·m)
SEBS1	6.25×10^3	5.21	2.77×10^5	12.53	
SEBS2	2.56×10^2	0.21	6.11×10^2	0.03	
SEB1	3.47×10^3	2.89	1.53×10^5	6.92	
SEB2	5.89×10^3	4.91	3.46×10^5	15.66	
PS	1.28×10^3	1.06	3.43×10^4	1.55	1.96
HDPE	1.20×10^3		2.21×10^4		1.96

[a] The η^* and G' data are the values at 50 s^{-1} from Figures 1 and 2. The torque values are for 50 rpm in the internal mixer.

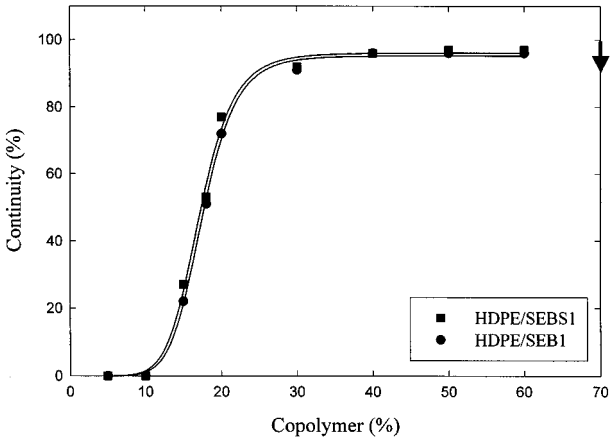

Figure 3. Percent continuity as a function of composition for HDPE/SEB1 and HDPE/SEBS1 blends. The arrow indicates the disintegration point for the two blend systems.

be closely related to the complex viscosity ratio from rheological equipment. The torque data are also reported in Table 2, and the torque ratio for PS/HDPE is 1.0. From the rheological curves shown in Figure 1, a complex viscosity ratio of 1 corresponds to a shear rate of 50 s^{-1}. At 50 s^{-1} the elasticity ratio from Figure 2 and Table 2 is 1.55.

3.2. Continuity Development and Pore Size. a. Compatible Binary System (Type I). Figure 3 shows the percent continuity as a function of blend composition for HDPE/SEB1 and HDPE/SEBS1 blends obtained after solvent extraction. The percent continuity of one of the components in a blend is defined as in eq 2. There is no continuity present at 10% copolymer for either of the blends. When the copolymer composition is increased to 18%, the level of continuity achieves 50% for both blends. An apparent cocontinuous structure is obtained in the range of 30−68% copolymer composition for both samples. Both blends disintegrated at 70% copolymer after extraction, indicating that complete phase inversion is achieved between a composition of 68−70%. It is interesting to note that both blends demonstrate a virtually identical percent continuity/composition relationship.

Cocontinuity in a binary blend system can be defined as the concentration range where both phases are 100% continuous. This is rigorously measured when selective solvents for each of the phases are available. In the case of HDPE/SEBS it is impossible to dissolve the HDPE without also dissolving out SEBS. For this reason we define a concentration region of apparent cocontinuity as existing from the onset of full continuity for SEBS (or SEB), using THF as a solvent, to the point at which the sample disintegrates in the presence of that same solvent. Sample disintegration in THF is a clear indication that SEBS (or SEB) is the matrix and HDPE is the dispersed phase. Although this approach likely overestimates the concentration range of dual-phase continuity, it should still allow for an effective comparison between the different interface types.

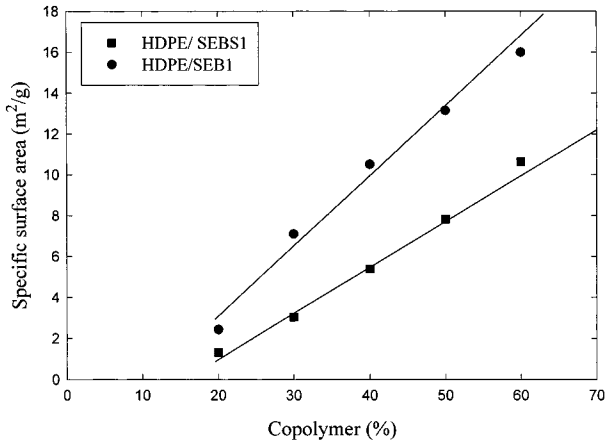

Figure 4. Dependence of specific surface area to copolymer amount for extracted HDPE/SEB1 and HDPE/SEBS1 blends.

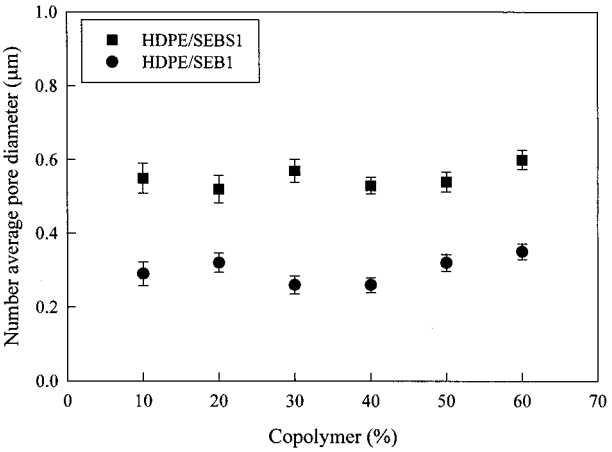

Figure 5. Pore size of extracted HDPE/SEB1 and HDPE/SEBS1 blends vs copolymer concentration.

The variation of specific surface area, as measured by the BET nitrogen adsorption technique, of HDPE/SEBS1 and HDPE/SEB1 with copolymer composition is shown in Figure 4. The specific surface area of both samples increases with increasing copolymer composition. The specific surface area of extracted 80HDPE/20SEBS1 is 1.32 m^2/g, while that of 80HDPE/20SEB1 is 2.43 m^2/g. The specific surface area for 40HDPE/60SEBS1 is 10.64 m^2/g and 16.00 m^2/g for 40HDPE/60SEB1. Clearly, the specific surface area of the SEB1 system is significantly higher than that of the SEBS1 system at the same copolymer concentration. Figure 5 illustrates pore diameters for both extracted compatible blend systems. The pore diameter is estimated from the specific surface area assuming a cylindrical pore shape as reported previously. [7] For the HDPE/SEBS1 blend the pore size is about 0.60 μm, while the pore size of the HDPE/SEB1 blend is only around 0.30 μm. HDPE/SEBS1 and HDPE/SEB1 clearly demonstrate little change in pore size with composition. It is interesting to observe that although the surface area of extracted HDPE/SEB1 increases about 10-fold with composition, there is little change in pore size. These results indicate that the effect of increasing composition in a compatible

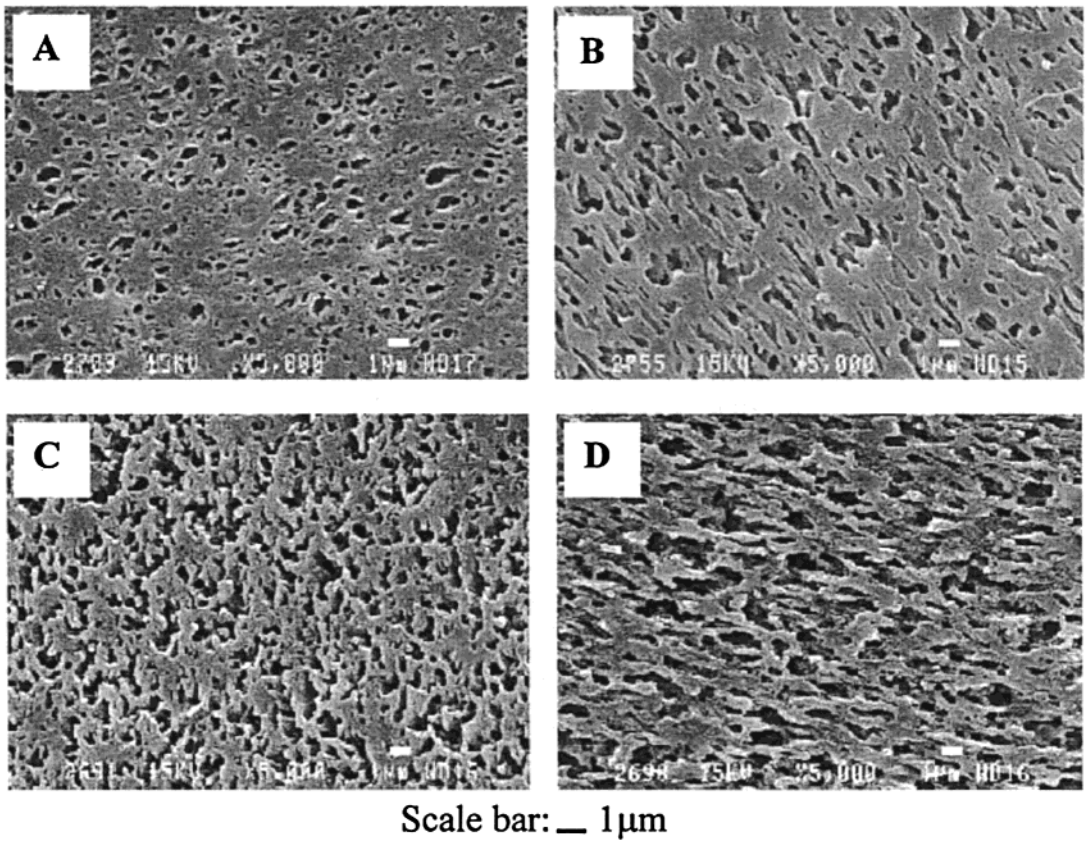

Figure 6. SEM micrographs for HDPE/SEBS1 blends at 195 °C: (A) 70 HDPE/30 SEBS1, (B) 60 HDPE/40 SEBS1, (C) 50 HDPE/50 SEBS1, and (D) 40 HDPE/60 SEBS1.

binary blend is to create a more dense continuous network of virtually equivalent pore size.

Figures 6 and 7 show SEM micrographs of both compatible binary blends in the composition range of 30−60% copolymer. As expected, the two-dimensional micrographs (Figures 6 and 7) are limited in their information related to dual-phase continuity (a three-dimensional structure); however, it is clear that a much finer microstructure is observed for the extracted blend containing diblock copolymer (HDPE/SEB1). It is also apparent that the pore size of each blend does not change significantly with concentration. Both these observations support the BET results from above.

b. Noncompatibilized Binary System (Type II) and Compatibilized Ternary System (Type III). The percent continuity/composition relationships for HDPE/SEBS1, HDPE/PS, and the HDPE/PS/SEBS1 blend systems are shown in Figure 8a,b. Figure 8b is an expanded view of the continuity development region.

For the noncompatible blend system (HDPE/PS), zero continuity was observed up to a PS concentration of 10%. The continuity of PS is 25% at 18% PS, and this increases to 84% at 30% PS. A fully continuous structure is obtained at about a volume concentration of 40% PS. This continuous structure disintegrates at 68% PS, once again indicating phase inversion. For the compatibilized ternary system (HDPE/PS/SEBS1), the continuity level is lower when compared with both the compatible and noncompatible binary systems at the same composition in Figure 8a,b. The compatibilized ternary blend system (HDPE/PS/SEBS1) displays zero continuity up to 15% PS. A level of 15% continuity is observed at 18% PS. The continuity increases to 80% at 30% PS, and a fully continuous structure is obtained at about 45% PS. The extracted structure disintegrates at 66% polystyrene. It is interesting to note that a narrowing of the cocontinuous range, as compared to the noncompatibilized binary blend, is observed for the compatibilized ternary system despite its low measured interfacial tension. An explanation of this effect will be elaborated on later in the discussion.

Figure 9 demonstrates the pore size/composition relationship for two compatible ternary systems. Very similar pore sizes are obtained for diblock or triblock modifiers, and very little change in pore size is observed with composition. Figure 10 illustrates the pore size/composition relationship for all the blend systems studied. For the noncompatible binary system (HDPE/PS), the pore size increases significantly with composition (from 2.0 μm at 10% PS to 6.3 μm at 60% PS). Depending on the type of interface, the scale of the microstructure can vary over almost 2 orders of magnitude. The pore size data were obtained from image analysis (when the minor phase was less than and equal to 30%) and with the BET technique (when the minor phase was equal to and above 30%). The good correspondence between the data from the two different techniques has been discussed in a previous publication.[7]

3.3. Influence of Diblock vs Triblock Copolymers on the Microstructure in the Compatible Binary Blends. As shown in Figure 9, the pore size of HDPE/SEB1 is about half that of HDPE/SEBS1. Table 2 indicates that the viscosity ratio between SEBS1 and SEB1 are different. To determine whether the viscosity ratio is controlling this observed effect on microstructure, blends with a high molecular weight diblock copolymer, SEB2 (M_n = 187 000, containing 26% sty-

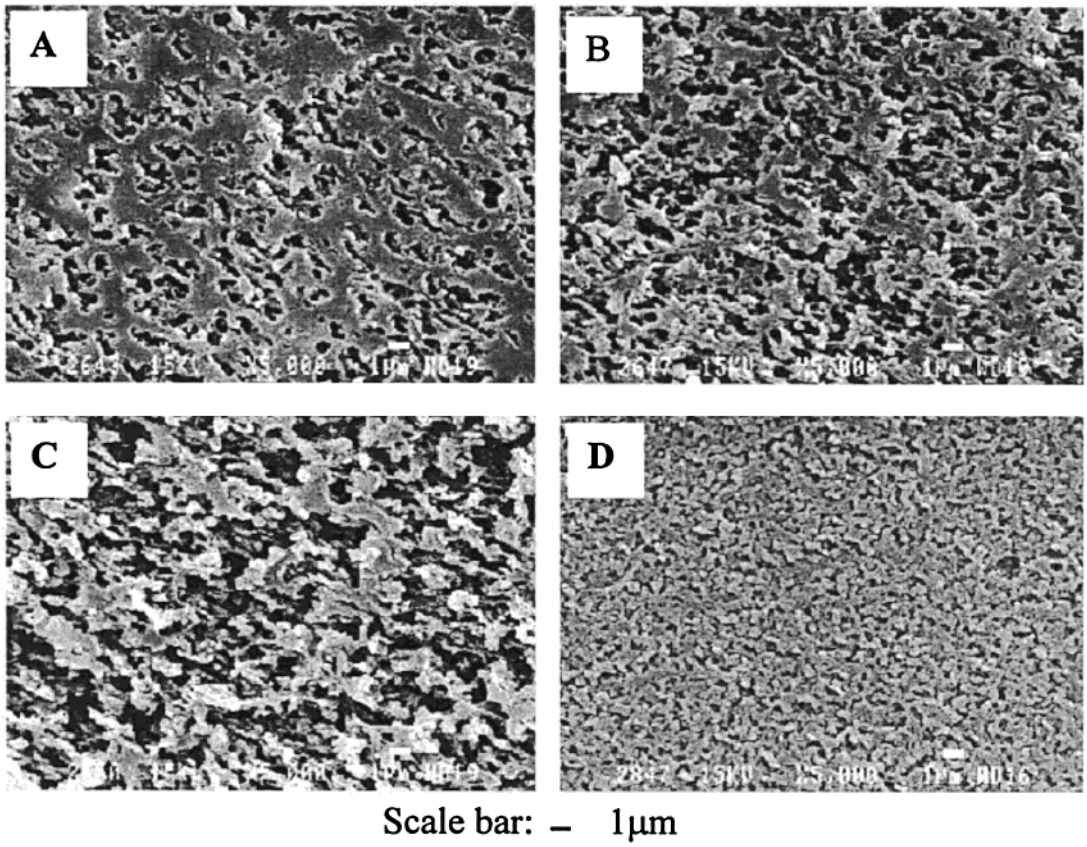

Figure 7. SEM micrographs for HDPE/SEB1 blends at 195 °C: (A) 70 HDPE/30 SEB1, (B) 60 HDPE/40 SEB1, (C) 50 HDPE/50 SEB1, and (D) 40 HDPE/60 SEB1.

Table 3. Rheological Properties and Specific Surface Area of HDPE/Copolymer Blends

blends	viscosity ratio at 50 s^{-1}	elasticity ratio at 50 s^{-1}	specific surf area (m^2/g)
50 HDPE/50 SEB1	2.89	6.92	13.15
40 HDPE/60 SEB1	2.89	6.92	16.00
50 HDPE/50 SEB2	4.91	15.66	10.74 (13.43)[a]
40 HDPE/60 SEB2	4.91	15.66	13.15 (15.23)[b]

[a] Corrected value (supposing that 100% of SEB2 is extracted). [b] Corrected value (supposing that 100% of SEB2 is extracted).

rene, referred to as SEB2), were prepared, and the specific surface area was tested. Table 3 lists the specific surface area of the samples. The 50 HDPE/50 SEB2 blend possesses a surface area of 10.74 m^2/g. It should be noted that in this case only 80% copolymer was removed (because of the high molecular weight of SEB2) during extraction, and a corrected value of 13.43 m^2/g based on 100% extraction was estimated. This is virtually identical to the surface area value for 50 HDPE/50 SEB1 (13.15 m^2/g). The specific surface area of 40 HDPE/60 SEB2 is 13.15 m^2/g. Considering that only 86% copolymer was removed (the same reason mentioned above) during extraction, a corrected value of 15.23 m^2/g based on 100% extraction was estimated. The corrected specific surface area of 40 HDPE/60 SEB2 is identical to the specific surface area of 40 HDPE/60 SEB1 (16.00 m^2/g) as well. Since surface area is related to pore size through volume fraction, these results clearly indicate that the viscosity ratio has little effect on microstructure in these low interfacial tension systems. This supports previous results on dispersed phase/matrix systems where the role of viscosity ratio on morphology was significantly moderated after addition of an interfacial modifier.[29] Having eliminated the possible influence of viscosity ratio, it appears that the finer structure of the HDPE/SEB1 blend, compared to HDPE/SEBS1 blend, is due primarily to the molecular architecture of the copolymer. A detailed explanation for this effect of architecture on microstructure is the subject of current study.

3.4. A Conceptual Mechanism for the Formation of Dual-Phase Continuity. a. Compatible Binary System (Type I). The compatible binary system possesses a low interfacial tension (interfacial tension is in the range between 0.7 and 1.0 mN/m). This low interfacial tension value (5 times less than the noncompatible binary system) results in a large capillary number:[31,32]

$$Ca = \frac{\eta_m \dot{\gamma} R}{\sigma} \tag{5}$$

where η_m is the matrix viscosity, σ is the interfacial tension, $\dot{\gamma}$ is the shear rate, and R is the radius of the drop. Such a system will also demonstrate long breakup times:[31,32]

$$t_b = \frac{2\eta_m R_0}{\Omega_m \sigma} \ln\left(\frac{0.82 R_0}{\alpha_0}\right) \tag{6}$$

where α_0 is the initial distortion amplitude, R_0 is the initial radius of the thread, and Ω_m is a function related to viscosity ratio. Evidence of long breakup times is shown in Figure 11 where it is demonstrated that HDPE/SEBS2 broke up only after 3 h under static conditions. Although static breakup of capillary instabilities is not the same as in the dynamic situation, it gives an indication of tendencies. Such a system should

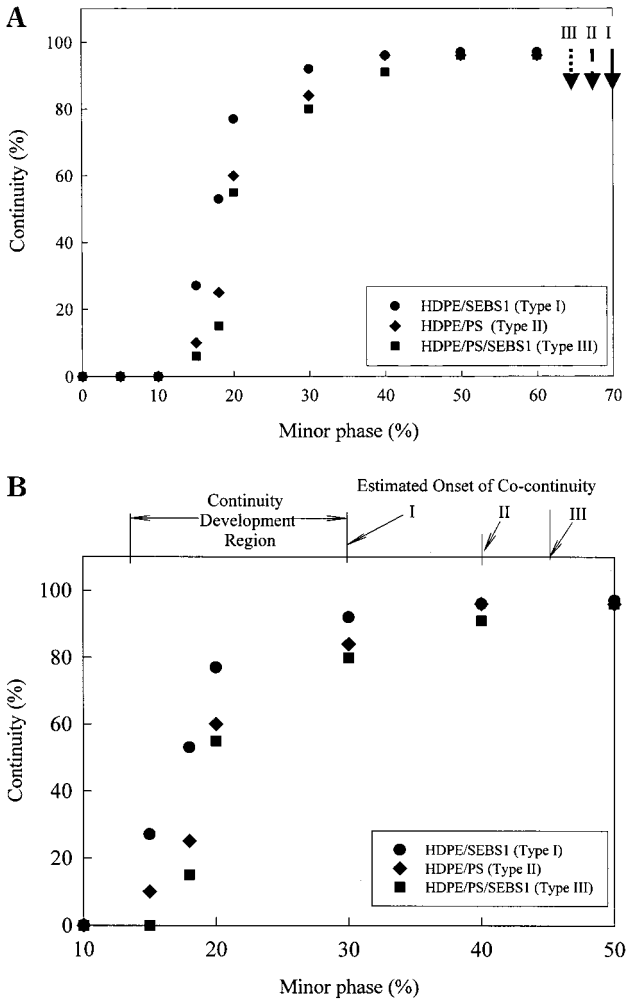

Figure 8. (A) Schematic illustration of continuity and dual-phase continuity development for three different blend systems: (I) compatible binary system, (II) noncompatible binary blend system, and (III) compatible ternary system. The arrows stand for the disintegration points for the three blend systems during extraction. HDPE/SEBS1 disintegrates at 70% SEBS1 (solid arrow), HDPE/PS at 68% PS (thick dash arrow), and HDPE/PS/SEBS1 at 66% PS (fine dash arrow). (B) Expanded view showing the percent continuity as a function of composition for HDPE/SEBS1, HDPE/PS, and HDPE/PS/SEBS1 blends.

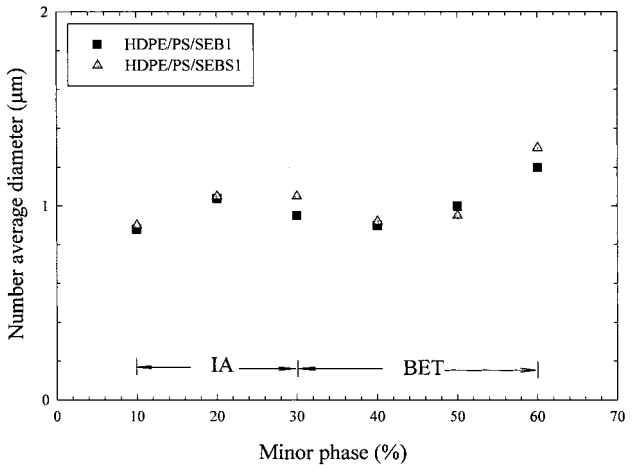

Figure 9. Pore size as a function of composition for HDPE/PS/SEBS1 and HDPE/PS/SEB1 blends. Twenty volume percent of compatibilizer is added based on the minor phase.

readily deform into a stable thread during melt mixing as observed by a number of authors.[12,13,25]

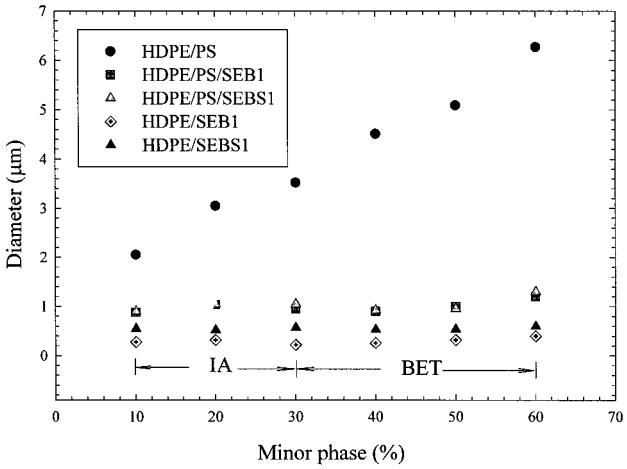

Figure 10. Pore size as a function of composition for HDPE/SEB1, HDPE/SEBS1, HDPE/PS, HDPE/PS/SEB1, and HDPE/PS/SEBS1 blends. Twenty volume percent of compatibilizer is added based on the minor phase.

Table 4. Breakup Time (t_b) and Interfacial Tension (σ) for HDPE/SEBS1, HDPE/SEBS2, PS/HDPE, and PA/SEBS2 Blends

matrix	thread	temp, °C	t_b, min	$q \times 10^2$	$\Omega \times 10^2$	σ (mN/m)
HDPE	SEBS2	195	180	0.183	20.9	0.72
SEBS1	HDPE	195		no distortion		
HDPE	PS	195	22	0.32	4.4	5.6
PA	SEBS2	250	4	2.10	3.37	12.7
SEBS2	PA	250	3	4.60	2.15	12.7

One needs to clearly address whether other factors, apart from the interface, are also seriously contributing to enhancing fiber stability in this study. We have demonstrated above that the viscosity ratio has little influence on microstructure in low interfacial tension binary blends, under these melt mixing conditions. Further support for this will be given later. Recently, Veenstra et al.[30] have speculated that when a copolymer is processed below its order−disorder transition, its stability as a fiber is enhanced. They demonstrate this clearly for a poly(ether−ester)/PS type polymer system by examining the breadth of the region of dual-phase continuity but in another paper[13] show only a very small apparent effect for SEBS Kraton copolymers blended with polypropylene. It appears that processing above or below the order−disorder transition showed only very little differences for SEBS type copolymers that had been rapidly quenched after processing.[13] They demonstrate more significant effects of order−disorder upon subsequent annealing. On the basis of that study, it is not likely that the order/disorder transition plays an important role in the fiber stability of the rapidly quenched HDPE/copolymer systems studied here.

To further demonstrate the dominant role of interfacial tension in controlling fiber stability during melt processing, we carried out a series of static fiber breakup experiments on an SEBS copolymer (SEBS2) that demonstrates Newtonian behavior (no yield stress, see Figure 1). Such a copolymer does not demonstrate an order−disorder transition. The results of the breakup experiment are shown in Table 4. For a thread of about 35 μm diameter an SEBS2 thread requires approximately 3 h to break up in the HDPE matrix (σ is 0.7 mN/m) at 195 °C. The breakup behavior of an SEBS2 thread sandwiched in HDPE films at 195 °C is illustrated in Figure 11. A PS thread in the same HDPE

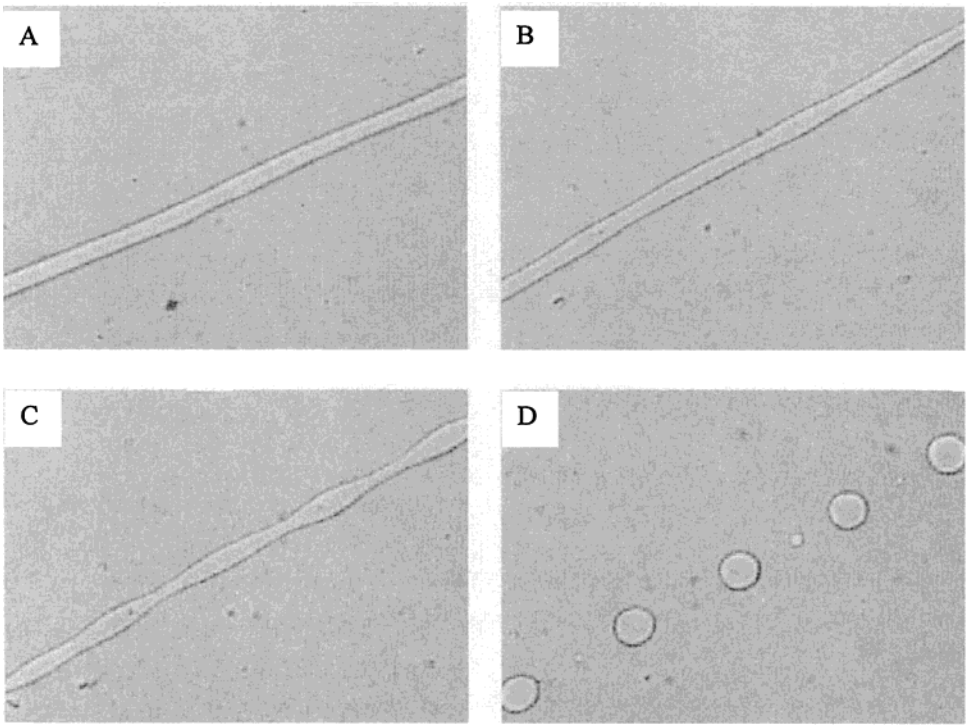

Figure 11. Static breakup process of an SEBS2 triblock copolymer thread imbedded in an HDPE matrix at 195 °C: (A) 30, (B) 90, (C) 120, and (D) 180 min.

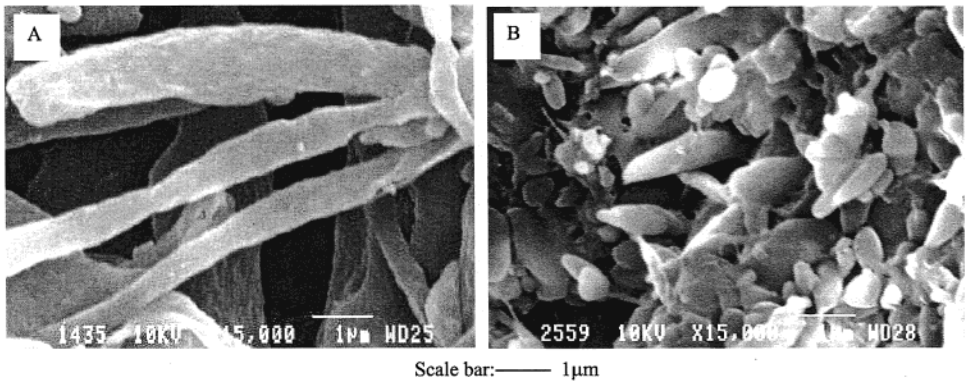

Figure 12. SEM photomicrographs of the dispersed HDPE phase after the matrix dissolution technique: (A) 5 HDPE/95 SEBS1 (Type I) and (B) 5 HDPE/95 SEBS2 (Type I).

matrix breaks up after 22 min (σ is 5.6 mN/m) at 195 °C. An SEBS2 thread in polyamide breaks up in approximately 4 min at 250 °C (σ is 12.7 mN/m). A HDPE thread in SEBS1 matrix does not show any distortion for about 5 h. The above strongly supports the concept of the dominant role of interfacial tension on fiber stability during melt mixing in the low interfacial tension HDPE/copolymer systems presented in the present work.

In such a case the thread lifetime during mixing is expected to be longer than the droplet lifetime even at low dispersed phase concentrations. Thread and droplet lifetimes can be defined as the time with which the particular shape is observed during the full course of melt mixing. The thread and droplet lifetimes can be directly related to the frequency at which they appear in blend systems. The longer the lifetime of the thread or droplet, the higher the respective frequencies.

Direct evidence of long thread lifetimes or higher frequencies at low dispersed phase concentration is demonstrated in Figure 12A where the matrix phase of the 5 HDPE/95 SEBS1 blend is dissolved away, and the dispersed phase is visualized by SEM after a combination of centrifugation and filtration as explained in the Experimental Section. The same procedure was applied to 5 HDPE/95 SEBS2, and the result is shown in Figure 12B. The micrograph of 5 HDPE/95 SEBS1 in Figure 12A clearly shows that the dispersed phase is in an elongated fiber form. It was impossible to carry out the 5 SEBS1/95 HDPE experiment since there was no way to dissolve the matrix without dissolving the dispersed phase. Nevertheless, all the features of low interfacial tension resulting in a high capillary number and long breakup times are present in the 5 HDPE/95 SEBS1 sample. In Figure 12B, for 5 HDPE/95 SEBS2, it can also be clearly seen that the dispersed phase is in an elongated fiber form. Note that Figure 12B represents a case of low viscosity ratio while Figure 12A represents the case of high viscosity ratio. These results clearly support, again, that in these very low interfacial tension systems interfacial tension phenomena dominate the fiber formation process.

In the case where the thread lifetime is greater than the droplet lifetime, continuity will develop principally

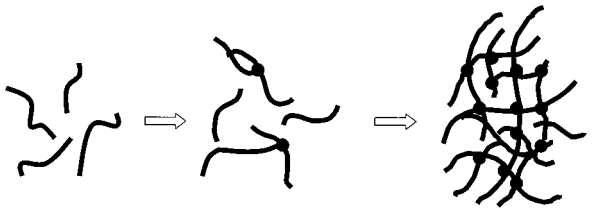

Figure 13. Schematic illustration of the development of cocontinuity via thread−thread coalescence. This phenomenon occurs when the thread lifetime is much greater than the droplet lifetime (at low dispersed phase volume fraction) during melt mixing.

through thread−thread coalescence. Figure 13 gives a schematic illustration of this process. For the case of stable threads, coalescence is limited locally to the crossover points as observed by Willemse et al.[12] This type of system would be expected to demonstrate the onset of percolation phenomena at low composition, full continuity of the minor phase would be attained at low composition, cocontinuity would be maintained over a wide composition range, and the pore size of the blend would change little with increasing minor phase concentration. Increasing the concentration would result in a more dense three-dimensional network of identical pore size. These expectations correlate with the experimental observations on every point.

b. Noncompatible Binary System (Type II). The noncompatible HDPE/PS binary blend system has a high interfacial tension of about 5.6 mN/m.[5] In such a case, droplet splitting, as opposed to capillary formation, should be a prominent mechanism.[31,32] Even if some capillary breakup does occur, the thread lifetime in this system would be substantially lower than the compatible binary system. It can be reasonably assumed for such a system at low concentration that the droplet frequency is greater than the thread frequency during melt mixing.

Direct evidence of the prominence of droplets at low concentration is demonstrated through the same matrix dissolution technique discussed above. Figure 14A clearly shows that in the 5 HDPE/95 PS blend a spherical dispersed phase morphology dominates. Fiber formation and continuity development in such a case are then principally developed through droplet−droplet coalescence. Figure 15 schematically demonstrates this process. A number of studies have shown the contribution of droplet−droplet coalescence to fiber formation for this interface type.[3,33] The expected features of such a system would be that percolation phenomena occur at higher composition than in Type I, full continuity would be maintained in a narrower composition range than in Type I, and the pore size of the blend would increase significantly with percent minor phase in the usual fashion[8,34,35] due to droplet−droplet coalescence. These expectations are consistent with the experimental observations for the Type II system.

c. Compatible Ternary System (Type III). The compatibilized ternary system (HDPE/PS/SEBS1) possesses a low static interfacial tension of about 1 mN/m. At first glance one might be tempted to analyze it in the same fashion as the compatible binary blend system. The situations, however, are not the same. During the melt mixing of a ternary system possessing an interfacial modifier, an initially interfacially saturated droplet is readily deformed; however, a fresh interface is developed during deformation. This situation is schematically illustrated in Figure 16. Under dynamic conditions if, for example, a spherical droplet deforms into an extended body with an aspect ratio of 4, that ellipsoid has 4 times more interfacial area than the equivalent volume sphere. If it is assumed that the time required to saturate the fresh thread interface is much greater than the thread breakup time, then the compatible ternary system actually more closely resembles the noncompatible binary case (droplet lifetime > thread lifetime) than the compatible binary one.

Direct evidence of the prominence of droplets at low concentration for the Type III interface system is demonstrated once again through the matrix dissolution technique. Figure 14B clearly shows that in the 5 HDPE/95 PS/20 SEBS1 blend a spherical dispersed phase morphology dominates. Fiber formation and continuity development in such a case will take place through droplet−droplet interactions. There is one major difference from the Type II case: the Type III droplet possesses interfacial modifier which results in a significant reduction in droplet−droplet coalescence. The effect of added interfacial modifier on coalescence reduction is a well-known phenomenon and has been studied extensively in the past.[34−38] The expected features for this case would be that percolation phenomena occur at higher composition than Type II due to diminished droplet−droplet coalescence; the region of dual-phase continuity should be narrower than Type II due to reduced droplet−droplet coalescence, and a low level of change of pore size with composition is expected due to reduced droplet−droplet coalescence. The overall pore size would be expected to be greater than Type I but less than Type II. Once again the experimental results are consistent with the expected features. A similar effect of delayed onset of percolation for a Type

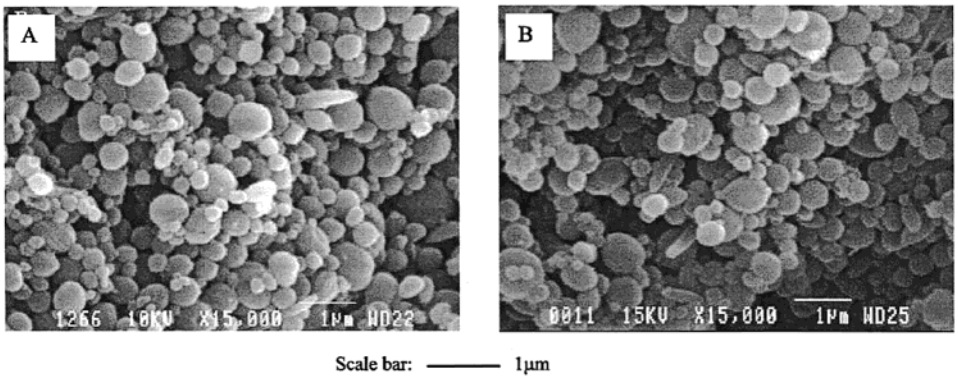

Figure 14. SEM photomicrographs of the dispersed HDPE phase after the matrix dissolution technique: (A) 5 HDPE/95 PS (Type II) and (B) 5 HDPE/95 PS/20 SEBS1 (Type III).

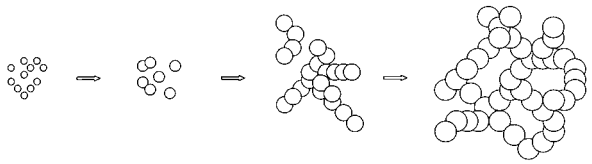

Figure 15. Schematic illustration of the development of the cocontinuity via droplet−droplet coalescence. This phenomenon takes place when the droplet lifetime is much greater than the thread lifetime (at low dispersed phase volume fraction) in a noncompatible binary blend system with high interfacial tension.

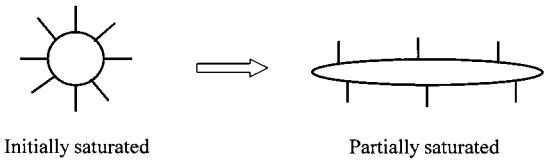

Figure 16. Schematic illustration of the deformation of the dispersed phase in a compatible ternary system. The saturated droplet saturated with interfacial modifier is deformed, and fresh interface is developed. If the time to emulsify the fresh interface is less than the time for breakup, then this system also represents the case of droplet lifetime greater than thread lifetime (at low dispersed phase volume fraction).

III system has also been observed by Bourry et al.[4] and was related to the suppression of coalescence in their cocontinuous HDPE/PS system in the presence of an interfacial modifier.

3.5. Thread Frequency Ratio. It is clear from the above discussion that the formation of stable fibers is critical to the development of continuity. Fiber formation, in turn, is developed through two basic routes: (1) single particle deformation/disintegration phenomena and/or (2) coalescence phenomena. In this paper the observed microstructural features indicate that fiber formation in the Type I system is dominated by deformation/disintegration and demonstrate that fiber formation in the Type II and III systems is dominated by droplet coalescence. It is also shown that the particular approach to achieving continuity has profound consequences on the scale of the resulting microstructure (Figure 10).

In this study the systems studied were chosen so as to define a clear distinction between the different interface types. The binary compatible blend possessed an interfacial tension about 5 times less than its binary incompatible counterpart. Also, a highly effective interfacial modifier was used for the compatible ternary system. (Static interfacial tension experiments demonstrate a 5-fold decrease in interfacial tension after addition of modifier.) In reality, however, when one considers all blends, a broad continuum/spectrum of interface types exists. For example, a variety of binary systems of varying compatibility is possible; incompatible binary systems of widely different interfacial tension are also possible. Also, a wide range of interfacial modifiers of varying efficacy is equally a possibility. Other factors that could potentially affect fiber formation during mixing are the type of flow field (an elongational flow field is much more effective in deforming the dispersed phase than shear flow fields) and possibly extreme viscosity ratios. Considering all the potential factors influencing fiber formation in polymer blends, it is clear that a basic parameter classifying the relative balance between fibers and droplets under any given condition would be very useful.

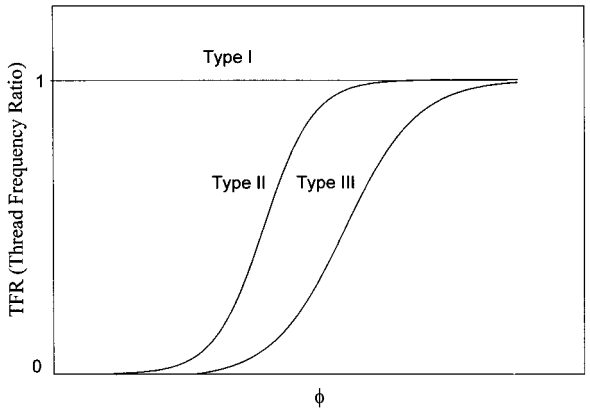

Figure 17. Idealized illustration of the thread frequency ratio vs volume fraction for the three types of blend interfaces.

To be able to better understand fiber formation in polymer blends, we define a thread frequency ratio (TFR) as

$$\mathrm{TFR} = \mathrm{tf}/(\mathrm{tf} + \mathrm{df}) \tag{7}$$

where tf is the thread frequency and df is the droplet frequency. TFR = 0 for a blend entirely composed of droplets, TFR = 1 for a blend entirely composed of fibers, and TFR = 0.5 indicates equal amounts of droplets and fibers. The dependence of TFR with concentration should be quite different for each of the three blend interface systems studied in this paper. In fact, by definition all types of polymer blends will demonstrate a TFR = 1 at some given concentration since all blends demonstrate cocontinuity. It is possible to trace the generalized dependence of the thread frequency ratio for the three different categories of polymer blend interfaces. This is shown in Figure 17. The Type I binary compatible blend will demonstrate a thread frequency ratio of 1, which is independent of concentration. (It should be noted that the onset of continuity can still be significantly influenced in the latter case by the extent of deformation, or aspect ratio, of a given system.) The Type II incompatible high interfacial tension blend would have a TFR at low concentrations equal to 0. As concentration increases and coalescence substantially contributes to fiber formation, a transition occurs, and the thread frequency ratio begins to tend toward 1. The Type III compatibilized ternary system will experience the transition from a TFR of 0 toward 1 at a higher concentration due to significantly reduced coalescence. In Figure 18, the matrix dissolution technique is used to demonstrate the influence of composition on the TFR for the HDPE/PS/SEBS1 system. A gradual increase in the TFR with composition is observed showing the expected trends for a system where cocontinuity development is dominated by droplet coalescence phenomena.

4. Conclusions

In this paper three different categories of blend interfaces are examined systematically in order to isolate the role of the interface in the development of cocontinuous morphologies during melt mixing. Depending on the interface type, the scale of the cocontinuous microstructure is found to vary over almost 2 orders of magnitude. Furthermore, high interfacial tension binary blends, Type II, demonstrate a strong dependence of scale with composition while the Type I and III inter-

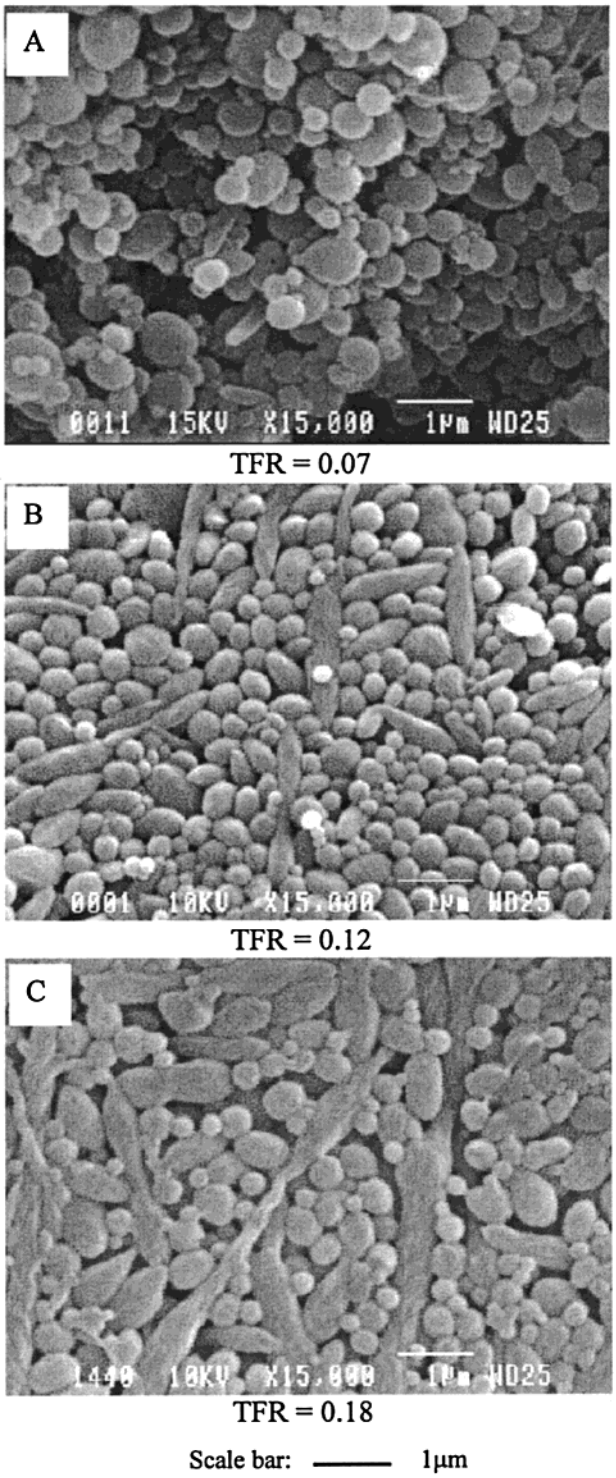

Figure 18. SEM photomicrographs of the dispersed HDPE phase and the corresponding TFR data after the matrix dissolution technique for a Type III system. Three dispersed phase concentrations are shown: (A) 5 HDPE/95 PS/20 SEBS1, (B) 10 HDPE/90 PS/20 SEBS1, and (C) 20 HDPE/80 PS/20 SEBS1.

faces possess cocontinuous microstructures where the pore size is virtually independent of composition. The interface type also has a stong influence on the breadth of the apparent region of dual-phase continuity with the widest range attributed to the Type I and the narrowest to Type III.

Using general arguments based on thread lifetime vs droplet lifetime during melt processing, a conceptual mechanism for the effect of the interface on dual-phase continuity formation is proposed. For the Type I binary system with low interfacial tension, the continuity development and microstructural features are consistent with a mechanism dominated by thread−thread coalescence (thread lifetime > droplet lifetime) since in that system the dispersed phase forms highly stable fibers during melt mixing. The formation and morphology of the cocontinuous Type II binary system with high interfacial tension are consistent with a mechanism controlled by droplet−droplet coalescence (droplet lifetime > thread lifetime). In the Type III system, continuity and microstructure are controlled by reduced droplet−droplet coalescence. This latter case is considered to be only partially compatibilized due to the generation of fresh interface during the deformation process, and hence it can be still be considered that the droplet lifetime is greater than the thread lifetime during melt mixing. Nevertheless, because of the partial emulsification, the droplet coalescence process is significantly reduced. This conceptual mechanism effectively explains all of the various experimental observations.

The relative presence of fibers or droplets during dynamic mixing is confirmed and analyzed quantitatively using a matrix dissolution/image analysis technique. A thread frequency ratio (TFR) is proposed as a basic general parameter to classify the relative presence of fibers to droplets during mixing and hence the type of continuity development and microstructure expected for a given system.

References and Notes

(1) Avgeropoulos, G. N.; Weissert, F. C.; Biddison, P. H.; Bohm, G. G. A. *Rubber Chem. Technol.* **1976**, *49*, 93.
(2) Jordhamo, G. M.; Manson, J. A.; Sperling, L. H. *Polym. Eng. Sci.* **1986**, *26*, 517.
(3) Favis, B. D.; Chalifoux, J. P. *Polymer* **1988**, *29*, 1761.
(4) Bourry, D.; Favis, B. D. *J. Polym. Sci., Polym. Phys.* **1998**, *36*, 1889.
(5) Mekhilef, N.; Favis, B. D.; Carreau, P. J. *J. Polym. Sci., Polym. Phys.* **1997**, *35*, 293.
(6) Mekhilef, N.; Verhoogt, H. *Polymer* **1996**, *37*, 4069.
(7) Li, J.; Favis, B. D. *Polymer* **2001**, *42*, 5047.
(8) Lyngaae-Jorgensen, J.; Utracki, L. A. *Makromol. Chem., Makromol., Symp.* **1991**, *48/49*, 189.
(9) Paul, D. R.; Barlow, J. W. *J. Macromol. Sci., Rev. Macromol. Chem.* **1980**, *C18*, 109.
(10) Utracki, L. A. *J. Rheol.* **1991**, *35*, 1615.
(11) Metelkin, V. I.; Blekht, V. S. *Colloid J. USSR* **1984**, *46*, 425.
(12) Willemse, R. C.; Posthuma de Boer, A.; Van Dam, J.; Gotsis, A. D. *Polymer* **1998**, *39*, 5879.
(13) Veenstra, H.; van Lent, B. J. J.; van Dam, J.; Posthuma de Boer, A. *Polymer* **1999**, *40*, 6661.
(14) Miles, I. S.; Zurek, A. *Polym. Eng. Sci.* **1988**, *28*, 796.
(15) Steinmann, S.; Gronski, W.; Friedrich, C. *Polymer* **2001**, *42*, 6619.
(16) Tchoudakov, R.; Breuer, O.; Narkis, M.; Siegmann, A. *Polym. Eng. Sci.* **1996**, *36*, 1336.
(17) Levon, K.; Marglina, A.; Patashinsky, A. Z. *Macromolecules* **1993**, *26*, 4061.
(18) Gubbles, F.; Jérôme, R.; Teyssié, Ph.; Vanlathem, E.; Deltour, R.; Calderone, A.; Parenté, V.; Brédas, J. L. *Macromolecules* **1994**, *27*, 1972.
(19) Verhoogt, H.; van Dam, J.; Posthuma de Boer, A. *Adv. Chem. Ser.* **1994**, *239*, 333.
(20) Elemans, P. H. M.; Janssen, J. M. H.; Meijer, H. E. H. *J. Rheol.* **1990**, *34*, 1311.
(21) Chapleau, N.; Favis, B. D.; Carreau, P. J. *J. Polym. Sci., Polym. Phys.* **1998**, *36*, 1947.
(22) Lepers, J.-C.; Favis, B. D. *J. Polym. Sci., Polym. Phys.* **1999**, *37*, 939.
(23) Willis, J. M.; Caldas, V.; Favis, B. D. *J. Mater. Sci.* **1991**, *26*, 4742.
(24) Rayleigh, L. *Proc. London Math. Soc.* **1879**, *10*, 4.
(25) Tomotika, S. *Proc. R. Soc. London* **1935**, *A150*, 322.

(26) Bourry, D. Master thesis, École Polytechnique de Montréal, Montréal, Canada, 1995.
(27) Saltikov, S. A. *Proceedings of the 2nd International Congress for Stereology*; Helias: New York, 1967.
(28) Favis, B. D. *Makromol. Chem., Macromol. Symp.* **1992**, *56*, 143.
(29) Fayt, R.; Jérôme, R.; Teyssié, Ph. *Makromol. Chem.* **1986**, *187*, 837.
(30) Veenstra, H.; Van Dam, J.; Posthuma de Boer, A. *Polymer* **1999**, *40*, 1119.
(31) Taylor, G. I. *Proc. R. Soc. London* **1932**, *A138*, 41.
(32) Taylor, G. I. *Proc. R. Soc. London* **1934**, *A146*, 501.
(33) Elmendorp, J. J.; Van der Vegt, A. K. *Polym. Eng. Sci.* **1986**, *26*, 1332.
(34) Fortelny, I.; Michalkova, D.; Koplikova, J.; Navratilova, E.; Kovar, J. *Angew. Makromol. Chem.* **1990**, *179*, 185.
(35) Fayt, R.; Jérôme, R.; Teyssié, Ph. *J. Polym. Sci., Polym. Lett.* **1986**, *24*, 25.
(36) Fayt, R.; Harrats, C.; Blacher, S.; Jérôme, R.; Teyssié, Ph. *Polym. Mater. Sci. Eng.* **1993**, *69*, 178.
(37) Matos, M.; Favis, B. D.; Lomellini, P. *Polymer* **1995**, *36*, 3899.
(38) Cigana, P.; Favis, B. D.; Jérôme, R. *J. Polym. Sci., Polym. Phys.* **1996**, *34*, 1691.

MA010104+